CSCanada
Energy Science and Technology
Vol. 4, No. 2, 2012, pp. 1-5
DOI:10.3968/j.est.1923847920120402.536

ISSN 1923-8460[PRINT]
ISSN 1923-8479[ONLINE]
www.cscanada.net
www.cscanada.org

Narrow Band Gap $AgInTe_2$ Solar Cells Fabricated by Printing Method

Duy-Cuong Nguyen[a]; Seigo Ito[a],*

[a]Department of Electrical Engineering and Computer Sciences, Graduate School of Engineering, University of Hyogo, Himeji, Hyogo 671-2280 Japan.
*Corresponding author.
Supported by the Innovative Solar Cells project (NEDO, Japan).

Received 22 February 2012; accepted 22 October 2012

Abstract
$AgInTe_2$ micron-particles were synthesized by mechanical ball milling method. Only $AgInTe_2$ phase was obtained in the powder after ball milling from the mixture of elements (Ag, In, and Te). $AgInTe_2$ particles had the variation in the size and the biggest particle was approximately 2 μm. $AgInTe_2$ solar cells were fabricated as <$AgInTe_2$/In_2S_3/TiO_2/FTO> superstrate structure by doctor-blade printing, and were annealed at various temperatures under nitrogen ambient. $AgInTe_2$ after annealing showed high crystallinity and two band gaps of 0.67 and 0.86 eV. Although no photocurrent was observed after annealing below 350 °C, the photocurrent was observed in $AgInTe_2$ superstrate solar cells after annealing over 400 °C. The short-circuit photocurrent density strongly increased up to 18 mA/cm^2 for the samples annealed at 600 °C for 5 min.
Key words: $AgInTe_2$; Solar cells; Printing method

Nguyen, D. C., & Ito, S. (2012). Narrow Band Gap $AgInTe_2$ Solar Cells Fabricated by Printing Method. *Energy Science and Technology*, *4*(2), 1-5. Available from: URL: http://www.cscanada.net/index.php/est/article/view/10.3968/j.est.1923847920120402.536
DOI: http://dx.doi.org/10.3968/j.est.1923847920120402.536

INTRODUCTION
Compound solar cellssuch as $CuInS(Se)_2$ (CIS), $Cu_2ZnSnS(Se)_4$ (CZTS), and $Cu_2InGaS(Se)_4$ (CIGS) have received many considerations from researcher around the world because their attractive properties as high light absorption coefficient and high efficiency (Jackson, P. *et al*., 2011; Barkhouse, D. A. R. *et al*., 2012; Repins, I. *et al*., 2008; Todorov, T. K. *et al*., 2010; Braunger, D. *et al*., 1996). In addition, compound solar cells can be fabricated by various methods including vacuum and non-vacuum methods. In order to improve the photoenergy conversion efficiency, tandem structures play important role, effectively. The best solar cell performed 43.5% conversion efficiency using such tandem structure (Green, M. A. *et al*., 2012). The goal of our research is development of narrow band gap compound absorber materials for applications in the bottom of tandem solar cells. Up to now, almost bottom cells in tandem solar cells use germanium, SiGe, or $In_{1-x}Ga_xAs$ (0.4-1.4) with band gap of 0.66, 0.66-1.2 or 0.4-1.4 eV, respectively, for absorber layer (Bett, A. W. *et al*., 2009; Shahrjerdi, D. *et al*., 2012; Maruyama, E. *et al*., 2002; Mc Cambridge, J. D. *et al*., 2011; Goh, E. S. M. *et al*., 2010). However, these materials have some drawbacks. $In_{1-x}Ga_xAs$ can be fabricated only by vacuum method and germanium is rather high cost. For these reason, we investigated $AgInTe_2$(AIT) for absorber layer in narrow band gap solar cells. According previous reports, the band gap of AIT is approximate 1 eV (Tell, B. *et al*., 1974); it is quite suitable for the bottom cells in the tandem solar cells. Mechanical ball-milling method has been well-known as simple method and easily to control the composition of elements in the compound. Hence, the mechanical ball-milling method was chosen for synthesizing AIT powder in this work.

The structural and optical properties of AIT powder synthesized by ball milling were analyzed in detail. The effect of annealing temperature on the photovoltaic properties and the crystallinity of AIT was thoroughly investigated.

1. EXPERIMENTAL
AIT powder was synthesized by mechanical ball milling method at a rotation speed of 700 rpm for 30 min. The

atomic ratio of starting materials of Ag, In, and Te is 1:1:2, respectively. The ball milling process was carried out in air ambient. Ag (purity of 99%, Chameleon Reagent), In (purity of 99.9%, Aldrich), and Te (99.9%, Kishida Chemical Co.) powders were utilized as starting materials.

The structure of AIT superstrate solar cells is described in Figure1. Transparent conducting oxides of florin-doped tin-oxide (FTO)-coated glass plates (Nippon Sheet Glass TEC-7, t = 2.2mm) were used as substrates. The TiO_2 compact and In_2S_3 buffer layers were deposited by spray pyrolysis method at 300 and 450 °C under air ambient, respectively; the process is similar to the previous report (Nguyen, D. C., & Ito, S., 2012). The solution for spraying the TiO_2 compact layer was a mixture of titanium acetylacetonate (TAA) and ethanol at an ethanol/TAA volume ratio of 9:1. The TAA solution was prepared by the slow injection of acetylacetone (purity of 99.5%, Kanto Chemical) into titanium tetraisopropoxide (purity of 97%, Kanto Chemical) with a mole ratio of 2:1. After TiO_2 compact layer deposition, samples were immersed into a 40 mM aqueous $TiCl_4$ aqueous solution at 70 °C for 30 min and washed with water and ethanol. The purpose of this process is to cap pin-holes in TiO_2 compact layers. For deposition of In_2S_3 buffer layers, a mixture of 10 mM $InCl_3$ (purity of 98%, Kishida Chemical Co.) and 20 mM thiourea (Tokyo Chemical Industry) in purified water was used. The thicknesses of TiO_2 compact and In_2S_3 buffer layers are 100 and 300 nm, respectively. AIT powder was mixed and grinded with propylene glycol in a mortar to make AIT paste. This paste was coated on In_2S_3/TiO_2/FTO by doctor-blade to form AIT absorber layers. After AIT doctor-blade, the samples were dried at 125 °C on a hot-plate.The samples were annealed at various temperatures for 30 min under nitrogen ambient. The cells were completed with molybdenum electrodes deposited by rf-magnetron sputtering. The size of the cells for photovoltaic measurement is 0.5 × 0.5 cm^2.

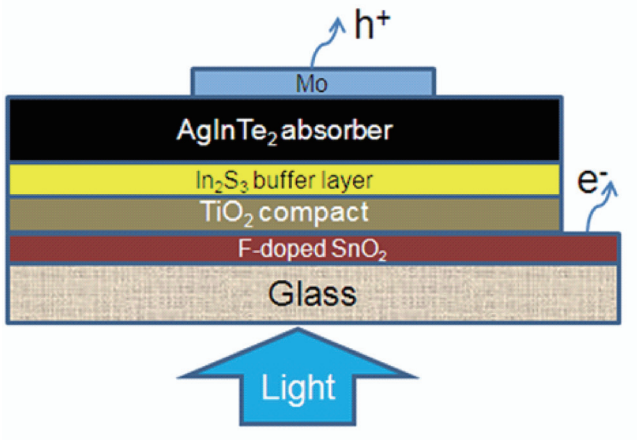

Figure 1
The Structure of AIT Superstrate Solar Cells

The size of AIT particles and thickness of the layers in the cells were confirmed by scanning-electron microscopy (SEM) (JSM-6510, JEOL). The phase structure and crystallinity of AIT were measured by x-ray diffraction (XRD) (Miniflex II, Rigaku) using CuK_α radiation. Absorption spectra were measured by an ultraviolet-visible spectroscopy (Lambda 750 UV/VIS Spectrometer, Perkin-Elmer). Photovoltaic measurements employed an AM 1.5 solar simulator equipped with a xenon lamp (Yamashita Denso YSS-100A). The power of the simulated light was calibrated to 100 $mWcm^{-2}$ using a reference Si photodiode (Bunkou Keiki). I-V curves were obtained by applying an external bias to the cell and measuring the generated photocurrent with a DC voltage current source (ADCMT 6240).

2. RESULTS AND DISCUSSION

Figure 2 shows SEM image and XRD pattern of AIT powder after ball milling at 700 rpm for 30 min. AIT powder includes particles with different size; the big particles are approximate 2 μm and the small one are around several hundred nanometer as shown in Figure 2(a). The XRD pattern of AIT powder was shown in Figure 2(b). The x-ray diffraction peaks were observed at the positions of 24.47, 40.42, 47.59, 63.75, and 72.97 degree. These peaks are of AIT phase, andcorrespond with the preferred orientations of (112), (204), (312), (413), and (421) (JDCPS, 1997; Jagomgi, A. *et al*., 2005). Several weak peaks were observed at the positions of around 30 degree; these peaks may be noise or the other phase. From XRD data, we can conclude that the powder after ball milling is mainly AIT. However, the appearance of noise in the XRD pattern also indicates the existence of amorphous state in AIT powder.

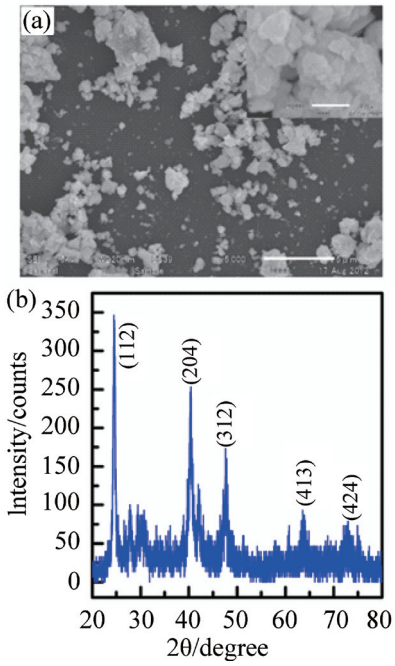

Figure 2
SEM Image (a) and XRD Pattern (b) of AIT Powder Ball-Milled at 700 rpm for 30 min Under Air Ambient

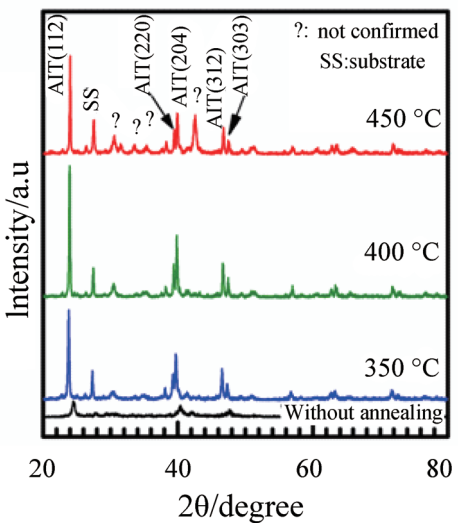

Figure 3
XRD Patterns of AIT Powder Without Annealing and AIT/In_2S_3/TiO_2/FTO with Annealing at 350, 400, and 450 °C for 30 min Under Nitrogen Ambient

In order to analyze the effect of annealing temperature on the microstructural, optical, and photovoltaic properties of AIT solar cells, AIT films printed on In_2S_3/TiO_2/FTO substrate were annealed at various temperature for 30 under nitrogen ambient. Figure 3 shows XRD patterns of AIT films with at without annealing. Although the annealing temperature is quite low (only 300 °C), XRD peaks of annealing samples drastically increased in comparison with non-annealing samples. In the range of 350-400 °C, peak intensity became stronger at higher annealing temperature.However, when annealing temperature increased up to 450 °C, the intensity of XRD peak was weaker and the several new weak peaks were observed at 33.58, 35.29, and 42.67 degree in AIT films. The appearance of the new peaks in AIT films indicates that the second phase, excepting AIT, was formed in the films, and is also reason for the reduction of AIT peaks. About the XRD peaks in Figure 3, it is very difficult to identify exactly, because of the mixtures of materials. Maybe, at 450 °C, the $AgInTe_2$ segregated to InTe and $AgTe_x$, and showed the several peaks in the XRD pattern. The XRD peaks around 30 degree may be related to InTe (JCPDS no. 81-1972, 77-2212), and around 30 and 40 degree may be related to $AgTe_x$, (JCPDS no. 27-0623, 21-1091, and 45-1305) respectively. The sharp and strong peaks observed at the annealed samples indicate that the crystallinity of AIT films was significantly improved, and AIT crystal particle size was bigger.

In order to analyze the effect of annealing temperature on the microstructure of AIT films, the cross-section of AIT/In_2S_3/TiO_2/FTO was observed by SEM. Figure 4 shows SEM cross-section image of AIT film annealed at 450 °C for 30 min and 600 °C for 5 min under nitrogen ambient. AIT films were fabricated by doctor-blade, so thickness of AIT films is rather thick, around 9 μm. AIT films is rather porous; it is difficult to find out the difference about macrostructure of AIT annealing at 450 and 600 °C. About SEM images in Figure 4, we want to just show the unchangeable structure at high temperature up to 600 °C. Hence, we did not put the images of 350 and 400 °C.

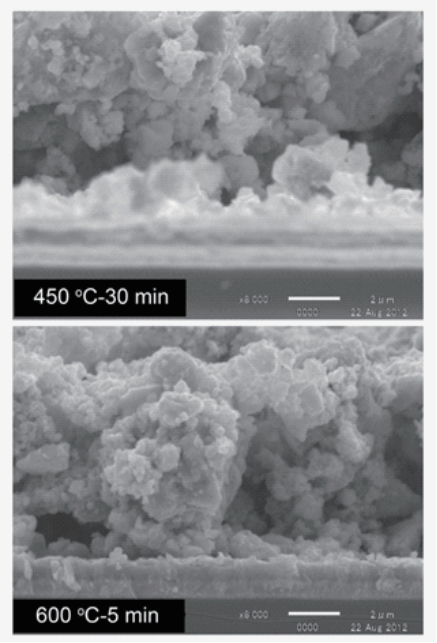

Figure 4
Cross-Section SEM Images of AIT/In_2S_3/TiO_2/FTO Annealing at 450 °C for 30 min and 600 °C for 5 min Under Nitrogen Ambient

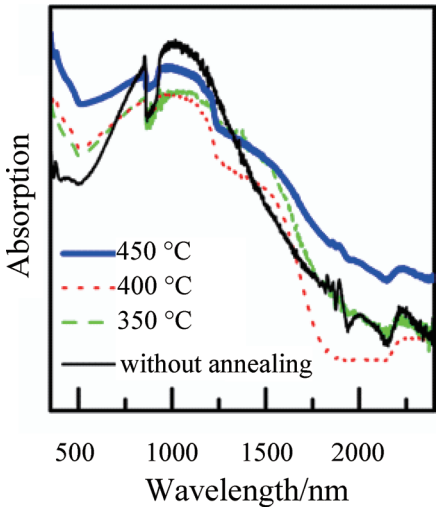

Figure 5
Absorption Spectra of AIT Powder Without Annealing and AIT/In_2S_3/TiO_2/FTO with Annealing at 350, 400, and 450 °C for 30 min Under Nitrogen Ambient

Figure 5 shows absorption spectra of AIT/In_2S_3/TiO_2/FTO without and with annealing at 350, 400 and 450 °C for 30 min under nitrogen ambient. In the case of AIT films without annealing, the slope of the spectrum was gentle. The gentle slope of non-annealing sample

may be due to the existence of amorphous state in AIT films as shown in XRD data in Figure 2(a). The slope of absorption spectra became sharply by annealing at 350 and 400 °C. The increase of the slope of absorption spectra can be attributed to the improvement of crystallinity in AIT films as shown in Figure 3. However, the slope became gentleby annealing from 400 to 450 °C. As shown in Figure 3, the strange peaks appeared at 450 °C. Therefore, we conjecture that the decrease of absorption spectra slope may be due the appearance of second phase in AIT films. The band gap of AIT films without annealing calculated from absorption spectrum is 0.69 eV. In the case of annealing samples, two absorption shoulders were observed in each AIT film. This indicates that two band gap exist in AIT. The band gaps of the annealed AIT films are 0.67 and 0.86 eV. The band gaps of AIT film obtained in this experiment are lower than previous report (approximate 1 eV) (Tell, B., *et al*., 1974). This difference may be due to high porosity in our AIT films as shown in Figure 4.

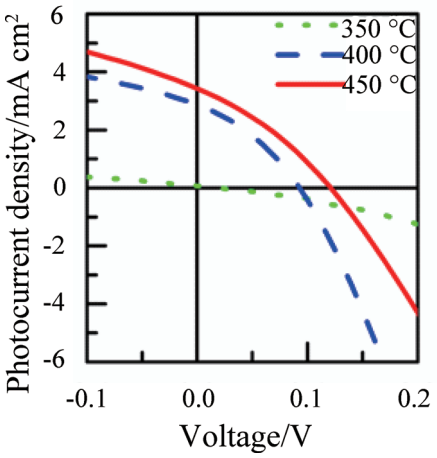

Figure 6
Photocurrent Density-Voltage Curves of AIT Solar Cells with Different Annealing Temperatures of 350, 400, and 450 °C for 30 min Under Nitrogen Ambient

Figure 6 shows photocurrent density-voltage curves of AIT solar cells with different annealing temperatures in the range of 350-450 °C for 30 min under nitrogen ambient. The photocurrent was not observed at the sample annealing at 350 °C. However, the photocurrent density increased with the increase of annealing temperature. The $AgInTe_2$ particle may need to melt each other to be a semiconductor layer, which may achieved over 400 °C. Therefore, the device annealed at 350 °C could not show the photocurrent in Figure 6. The short-circuit photocurrent density, open-circuit voltage, fill factor, and conversion efficiency of the sample annealed at 450 °C are 3.4 mA/cm^2, 0.12 V, 0.32, and 0.13%, respectively. The short-circuit photocurrent density obtained at the sample annealed at 400 and 450 °C is rather low. The key point to get high photocurrent density in solar cells is big grain in absorber layers. However, in this case, a lot of AIT small particles existed in the absorber layer and AIT films is rather highly porous as shown in Figure 4; this is reason for getting low short-circuit photocurrent density as mentioned above.

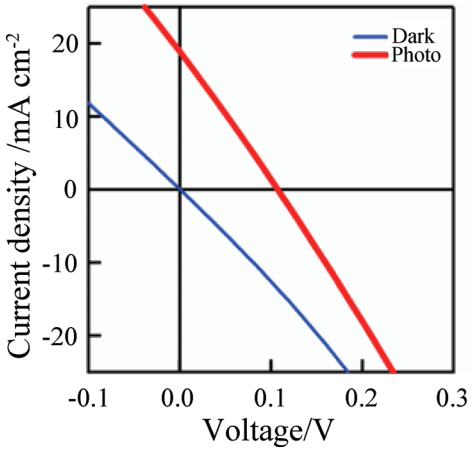

Figure 7
Current Density-Voltage Curves of AIT Solar Cell in Dark and Light with Annealing Temperature of 600 °C for 5 min Under Nitrogen Ambient

In order to improve the short-circuit photocurrentdensity, AIT samples were annealed at 600 °C for 5 min under nitrogen ambient. About photo I-V response, the photocurrent using the device annealed at 600 °C produce high photocurrent of 20 mA/cm^2, which is 5 times higher than that at 450 °C. Hence, the data were shown in Figure 6 and 7, separately. In this case, the annealing time was shorter than the samples were annealed at 350, 400 and 450 °C, because In_2S_3 buffer layer is rather unstable at high annealing temperature. The photocurrent density-voltage curve was shown in Figure 7. The cell parameters are short-circuit photocurrent density of 18 mA/cm^2, open-circuit voltage of 0.1 V, fill factor of 0.25, and conversion efficiency of 0.52%. The fill factor is rather low, only 0.25; thereason may be due to the instability of In_2S_3 buffer layer at high temperature (Nakada, T., *et al*., 1998).

CONCLUSIONS

AIT powder was synthesized by mechanical ball milling method at rotation speed of 700 rpm for 30 min under air ambient. XRD pattern showed that the powder obtained after ball milling includes AIT crystallites and amorphous state. AIT films showed narrow band gaps of 0.67 and 0.86 eV; these band gaps are quite appropriate for applications in the bottom cell of tandem solar cells. Although AIT films after annealing showed rather porously, a photocurrent was observed in AIT solar cells. The parameters of the best cell are 18 mA/cm^2 short-circuit photocurrent density, 0.1 V open-circuit voltage, 0.25 fill factor, and 0.52% conversion efficiency. According to these results, AIT is really potential candidate for narrow band gap solar cells.

REFERENCES

[1] Jackson, P., Hariskos, D., Lotter, E., Paetel, S., Wuerz, R., Menner, R., Wischmann, W., & Powalla, M. (2011). New World Record Efficiency for Cu(In,Ga)Se_2 Thin-Film Solar Cells Beyond 20%. *Prog. Photovolt: Res. Appl.*, *19*(7), 894-897.

[2] Barkhouse, D. A. R., Gunawan, O., Gokmen, T., Todorov, T. K., & Mitzi, D. B. (2012). Device Characteristics of a 10.1 % Hydrazine-Processed $Cu_2ZnSn(Se,S)_4$ Solar Cell. *Prog. Photovolt: Res. Appl.*, *20*(1), 6-11.

[3] Repins, I., Contreras, M. A., Egaas, B., DeHart, C., Scharf, J., Perkins, C. L., To, B., & Noufi, R. (2008). 19.9%-Efficient ZnO/CdS/$CuInGaSe_2$ Solar Cell with 81.2% Fill Factor. *Prog. Photovolt: Res. Appl.*, *16*(3), 235-239.

[4] Todorov, T. K., Reuter, K. B., & Mitzi, D. B. (2010). High-Efficiency Solar Cell with Earth-Abundant Liquid-Processed Absorber. *Adv. Mater.*, *22*(20), E156-E159.

[5] Braunger, D., Hariskos, D., Walter, T., & Schock, H. W. (1996). An 11.4% Efficient Polycrystalline Thin Film Solar Cell Based on $CuInS_2$ with a Cd-Free Buffer Layer. *Sol. Energy Mater. Sol. Cells*, *40*(2), 97-102.

[6] Green, M. A., Emery, K., Hishikawa, Y., Warta, W., & Dunlop, E. D. (2012). Solar Cell Efficiency Tables (Version 40). *Prog. Photovolt: Res. Appl.*, *20*(5), 606-614.

[7] Bett, A. W., Dimroth, F., Guter, W., Hoheisel, R., Oliva, E., Phillips, S. P., Schone, J., Siefer, G., Steiner, M., Wekkeli, A., Welser, E., Meusel, M., Kostler, W., & Strobl, G. (2009). Highest Mutli-Junction Solar Cell for Terrestrial and Space Application. The 24th European Photovoltaic Solar Cell Conference and Exhibition, 21-25 September 2009, Hamburg, Germany.

[8] Shahrjerdi, D., Bedell, S. W., Ebert, C., Bayram, C., Hekmatshoar, B., Fogel, K., Lauro, P., Gaynes, M., Gokmen, T., Ott, J. A., & Sadana, D. K. (2012). High-Efficiency Thin-Film InGaP/InGaAs/Ge Tandem Solar Cells Enabled by Controlled Spalling Technology. *Appl. Phys. Lett.*, *100*(5), 053901.

[9] Maruyama, E., Okamoto, S., Terakawa, A., Shinohara, W., Tanaka, M., & Kiyama, S. (2002). Toward Stabilized 10% Efficiency of Large-Area (>5000 cm^2) a-Si/a-SiGe Tandem Solar Cells Using High-Rate Deposition. *Sol. Energy Mater. Sol. Cells*, *74*(1-4), 339-349.

[10] Mc Cambridge, J. D., Steiner, M. A., Unger, B. L., Emery, K. A., Christensen, E. L., Wanlass, M. W., Gray, A. L., Takacs, L., Buelow, R., McCollum, T. A., Ashmead, J. W., Schmidt, G. R., Haas, A. W., Wilcox, J. R., Meter, J. V., Gray, J. L., & Moore, D. T. (2011). Compact Spectrum Splitting Photovoltaic Module Withhigh Efficiency. *Prog. Photovolt: Res. Appl.*, *19*(3), 352-360.

[11] Goh, E. S. M., Chen, T.P., Sun, C.Q., & Liu, Y.C. (2010). Thickness Effect on the Band Gap and Optical Properties of Germanium Thin Films. *J. Appl. Phys.*, *107*(2), 024305.

[12] Retrieved from http://en.wikipedia.org/wiki/Indium_gallium_arsenide

[13] Tell, B., Shay, J. L., & Kasper, H. M. (1974). Some Properties of $AgA1Te_2$, $AgGaTe_2$, and $AgInTe_2$. *Physical Review B*, *9*(12), 5203.

[14] Nguyen, D. C., & Ito, S. (2012). Superstrate $CuInSe_2$-Printed Solar Cells on In_2S_3/TiO_2/FTO/Glass Plates. *Energy Science and Technology*, *3*(2), 10-17.

[15] Joint Committee for Powder Diffraction Standards, Powder Diffraction File. No. 85-1575 (JDCPS International Center Diffration Data, 1997).

[16] Jagomgi, A., Krustok, J., Raudoja, J., Grossberg, M., Oja, I., Krunks, M., & Danilson, M. (2005). Photoluminescence and Raman Spectroscopy of Polycrystalline $AgInTe_2$. *Thin Solid Films*, *480-481*(1), 246-249.

[17] Nakada, T., Kume, T., & Kunioka, A. (1998). Superstrate-Type $CuInSe_2$-Based Thin Film Solar Cells by a Low-Temperature Process Using Sodium Compounds. S*ol. Energy. Mater. Sol. Cells*, *50*(1-4), 97-103.